Three-Dimensional Analysis of Ice Sheet Indentation: Lower-Bound Solutions

D. G. Karr
Massachusetts Institute of Technology,
Cambridge, Mass. 02139

The methods of plastic limit analysis are used to determine the indentation pressures of a flat rigid punch on a columnar ice sheet. The ice sheet is idealized as a semi-infinite layer of elastic-perfectly plastic material. Representative strength parameters of columnar sea ice are used to define anisotropic yield criteria for the ice sheet. The anisotropic yield criteria reflect the variations in mechanical properties caused by the horizontal orientation of the c-axis of sea ice in the columnar zone. Numerical results are obtained by applying the lower-bound theorem of plastic limit analysis. A three-dimensional stress field is optimized for a given ice condition for various indentor sizes. The effects of varying the aspect ratio (defined as the ratio of indentor width to ice thickness) are then addressed. A comparison of results for intermediate aspect ratios to results for extremely high (plane stress) and extremely low (plane strain) aspect ratios is presented. It is found that the transition from plane stress to plane strain is governed by the tensile strength of the ice medium.

Introduction

The methods of plastic limit analysis are used to calculate the pressures required to indent an ice sheet. Lower-bound solutions are obtained by optimizing a three-dimensional stress field in order to determine the indentation pressures which cause yielding of the ice medium. The numerical results thus indicate the minimum loads required to initiate penetration of the indentor into the edge of the ice sheet. The failure mechanism of the ice is assumed to be purely plastic deformation and the conditions of the lower-bound theorem are thus strictly satisfied.

The failure envelopes or yield criteria used to describe ice strength are highly dependent upon strain rate. The use of a particular failure envelope thus corresponds to a given ice type, temperature and strain rate. The Von Mises and the Drucker-Prager yield criteria are used to compare the three-dimensional lower-bound results to previous limit analysis results obtained using these criteria. Anisotropic criteria, applicable to columnar sea ice are also used to study the effects of indentation aspect ratios.

The stress field addressed in this study includes a rigorous three-dimensional elasticity solution for a semi-infinite sheet subjected to a distributed edge load. For certain stress states and higher strain rates, the failure envelope for ice may actually correspond to fracture rather than ductile flow. Thus, a knowledge of the state of stress in the sheet in the elastic range provides much insight as to the expected modes of failure of the ice. This also provides a means of assessing the limitations of the assumption of plastic deformation.

Contributed by the OMAE Division and presented at the 5th International Symposium and Exhibit on Offshore Mechanics and Arctic Engineering, Tokyo, Japan, April 13–22, 1986, of THE AMERICAN SOCIETY OF MECHANICAL ENGINEERS. Revised manuscript received by the OMAE Division, June 17, 1987.

Material Idealization

The fracture and plastic flow characteristics of ice is dependent upon the state of stress, substructure, temperature and strain rate. In this study, ice is considered as an elastic-perfectly plastic material. The stress-strain diagram consists of an initial straight line with stress directly proportional to strain and a post failure line of constant stress. The yield criterion defines the stress state for transition from elastic to perfectly plastic deformation.

In the columnar zone of an ice sheet the c-axes of the ice crystals are generally randomly oriented in the plane of the ice sheet [1]. The mechanical properties are then isotropic in the plane of the sheet. The degree of elastic anisotropy, which is caused by the preferred orientation of the c-axes, is expected to vary from about 10 to 30 percent, depending on the state of stress [2]. This elastic anisotropy is ignored in determining the three-dimensional elasticity solutions. The anisotropic nature of the failure of the ice, however, is incorporated in the selected yield functions.

The Von Mises yield criterion is first used in order to provide a direct comparison with previous three-dimensional upper-bound solutions. This criterion is isotropic and in principal stress space defines a circular cylinder [3], given by

$$J_2 = \tfrac{1}{6}[(S_1 - S_2)^2 + (S_2 - S_3)^2] + (S_3 - S_1)^2] = K^2 \quad (1)$$

where J_2 is the second invariant of the deviatoric stress tensor, S_1, S_2, and S_3 are the principal stresses [4], and K is a strength parameter constant.

The Von Mises criterion indicates that material yield is independent of hydrostatic stress and does not, in general, accurately reflect the strength of ice. However, if the effective strain rates are very low, there is no significant difference between tensile strength and compressive strength [5]. The Von Mises criterion may then be adequate for these limited conditions provided there is no significant anisotropy.

Drucker and Prager [6] suggested a generalized Von Mises function often used in soil mechanics, defined by

$$\alpha I + J_2^{1/2} = K \tag{2}$$

where I is the sum of principal stresses and α and K are constants. This criterion is used in the following to address the effects of hydrostatic stress on indentation pressures. The sensitivity of failure to hydrostatic stress is reflected by the coefficient α, and for $\alpha = 0$ reduces to the Von Mises criterion.

In the following indentation study, it is convenient to normalize the stresses with respect to the absolute value of the uniaxial compression strength, C_o. The normalized Drucker-Prager yield condition is then

$$\alpha \bar{I} + J_2^{1/2}/C_o = \sqrt{3}/3 - \alpha \tag{3}$$

where $\bar{I} = I/C_o$. Note that the Drucker-Prager criterion is a two-parameter function, and normalizing the stresses with respect to C_o requires the relation

$$K = (\sqrt{3}/3 - \alpha)C_o \tag{4}$$

By forcing the uniaxial compression strength to be properly reflected, a single independent parameter, α, is required to define the yield function. As is discussed later, two important characteristics of a particular yield function are the uniaxial tension strength and the confined compression strength. If the uniaxial tension strength is used to determine the value for α, then the confined compression strength is also determined. For a given uniaxial compression strength, as the tensile strength decreases the confined compression strength necessarily increases. For indentation problems this is often a crucial limitation of the Drucker-Prager criterion.

Finally, an anisotropic failure criterion is used to describe the failure envelope of columnar sea ice. Reinicke and Ralston [7] suggested a special case of Pariseau's n-type yield function [8] in the form

$$\begin{aligned} f = {} & a_1[(\sigma_y - \sigma_z)^2 + (\sigma_x - \sigma_z)^2] \\ & + a_3(\sigma_x - \sigma_y)^2 + a_4(\tau_{xz}^2 + \tau_{yz}^2) \\ & + a_6\tau_{xy}^2 + a_7(\sigma_x + \sigma_y) + a_9(\sigma_z) - 1 \\ = {} & 0 \end{aligned} \tag{5}$$

where σ and τ denote normal and shear stresses, respectively, a_1, a_3, a_4, a_7 and a_9 are coefficients and $a_6 = 2(a_1 + 2a_3)$. The material so described is isotropic in the x-y plane which is the plane of the ice sheet for the cases discussed in this paper. The anisotropic yield function for columnar sea ice is then defined by 5 independent material strength coefficients.

Normalizing the stresses with respect to the uniaxial compression strength, C_o, yields

$$\begin{aligned} f = {} & \bar{a}_1[(\bar{\sigma}_y - \bar{\sigma}_z)^2 + (\bar{\sigma}_x - \bar{\sigma}_z)^2] \\ & + a_3(\bar{\sigma}_x - \bar{\sigma}_y)^2 + \bar{a}_4(\bar{\tau}_{xz}^2 + \bar{\tau}_{yz}^2) \\ & + \bar{a}_6\bar{\tau}_{xy}^2 + \bar{a}_7(\bar{\sigma}_x + \bar{\sigma}_y) \\ & + \bar{a}_9(\bar{\sigma}_z) - 1 \\ = {} & 0 \end{aligned} \tag{6}$$

where $\bar{\sigma} = \sigma/C_o$, $\bar{\tau} = \tau/C_o$ and

$$\begin{aligned} \bar{a}_1 &= a_1C_o^2, \quad \bar{a}_3 = a_3C_o^2, \\ \bar{a}_4 &= a_4C_o^2, \quad \bar{a}_6 = a_6C_o^2, \\ \bar{a}_7 &= a_7C_o, \quad \bar{a}_9 = a_9C_o \end{aligned}$$

Forcing the yield function to properly reflect uniaxial compression requires

$$\bar{a}_7 = \bar{a}_1 + \bar{a}_3 - 1 \tag{7}$$

Equation (6) is used in the following indentation analysis. In addition to being able to reflect anisotropic strength characteristics, it is also somewhat more flexible in describing various shapes of the failure envelope. For example, for conditions of plane stress, various ratios of uniaxial tension and confined compression strength can be achieved. Reinicke and Ralston [7], Ralston [9], and Timco and Frederking [10] describe methods for determining the coefficients of equation (5).

Limit Analysis

In plastic limit analysis, the limit load is defined as the plastic collapse load of an ideal body which has the following properties [11]: (*a*) the material exhibits perfect plasticity, (*b*) the yield surface is convex, and (*c*) changes in geometry of the body at the limit load are negligible. Given such a material, the lower-bound limit theorem is stated as [12]:

> Collapse will not occur if any state of stress can be found which satisfies equilibrium and the boundary conditions on stress and for which all stress points lie inside the yield surface.

Determining lower-bound solutions for the indentation problem thus involves determining stress fields within the material which satisfies equilibrium and the boundary condition throughout the material without violating the yield criterion. Discontinuous stresses are permitted provided equilibrium is maintained. This proves to be highly useful as will be discussed in the following sections.

Three-Dimensional Stress Field

Consider now a semi-infinite plate subjected to a distributed load induced by contact of an indentor as shown in Fig. 1. The plate lies on the x-y plane with the origin located at the center of the plate's edge. The plate thickness is $2c$ and the width of the contact zone is $2b$.

A three-dimensional elasticity solution for the stresses through the sheet is first obtained by assuming a uniform pressure over the entire contact area. The elasticity solution satisfies equilibrium and the boundary conditions at all points. This solution is based on the generalized theory of plane stress proposed by Clark and Reissner [13]. Clark [14] applied this three-dimensional correction theory for the case of a sinusoidally varying normal edge load acting parallel to the plane of the sheet. The edge stress is distributed uniformly along the plate thickness. The normal edge stress is then given by

$$\sigma_y = \bar{\sigma}_o \cos \bar{\alpha}x$$

where $\bar{\sigma}_o$ is a constant and $\bar{\alpha} = 2\pi/1$, where 1 is the periodic length. The three-dimensional stresses have the approximate

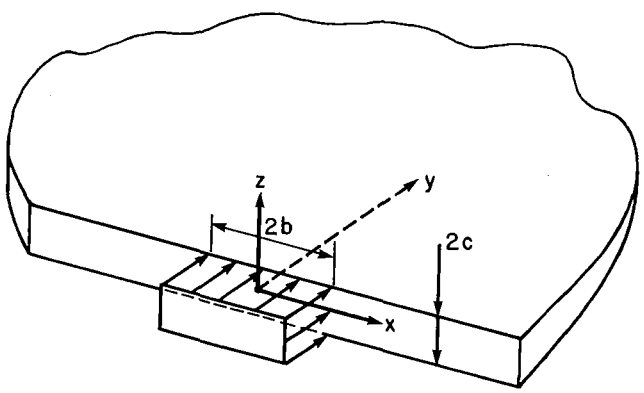

Fig. 1 Indentation geometry for a semi-infinite sheet

form

$$\sigma_x, \sigma_y, \tau_{xy}) = \frac{(N_{xx}, N_{yy}, N_{xy})}{2c} + \frac{R_{xx}, R_{yy}, R_{xy})}{2c} Z''(z) \quad (8)$$

$$(\tau_{xz}, \tau_{yz}) = \frac{(S_x, S_y)}{2c} Z'(z) \quad (9)$$

$$\sigma_z = -\frac{T}{2c} Z(z) \quad (10)$$

where

$$Z_{(z)} = -\frac{c^2}{4}\left(1 - \frac{Z^2}{c^2}\right)^2 \quad (11)$$

and Z' and Z'' are the first and second derivatives of Z with respect to z. The stress resultant quantities, $Nxx, \ldots . T$ are functions of the coordinates x and y. This form of the linear elastic solutions is consistent with the three-dimensional equilibrium equation boundary conditions. Using the solutions provided by Clark for the sinusoidal normal edge load, solutions are obtained for uniformly distributed load by means of a Fourier series.

The periodic system shown in Fig. 2 is approximated by the Fourier series

$$f(x) = \frac{2b}{T} + \sum_{n=1}^{\infty} \frac{2}{n\pi} \sin\left(\frac{2n\pi b}{T}\right)\cos\left(\frac{2n\pi}{T}x\right) \quad (12)$$

where T is the period of the system. Note that the period must be long enough such that in regions near the applied load, the effects of the adjacent applied loads are negligible. With a system period of $T = 10b$, several terms (approximately 40) must be used to closely approximate the desired stress distribution. In this analysis a period of $10b$ is normally adequate although for higher values of c/b the period must be increased. In fact as plane strain conditions are approached, the ratio c/b approaches infinity and this method becomes difficult to apply since more terms in the Fourier series are required.

It is convenient to normalize the distance parameters with respect to the indentor half-width b; that is, let

$$\bar{x} = x/b, \quad \bar{y} = y/b, \quad \bar{z} = z/b, \quad \bar{c} = c/b \quad (13)$$

Also, by normalizing the natural period $\gamma = T/b$ and letting $\bar{\gamma} = 1/\gamma$, then equation (12) takes the form

$$f(x) = 2\bar{\gamma} + \sum_{n=1}^{\infty} \frac{2}{n\pi} \sin(2n\pi\bar{\gamma})\cos(2n\pi\bar{\gamma}\bar{x}) \quad (14)$$

As an example of this technique, the Fourier series expansion for a distributed indentor pressure of σ is shown in Fig. 3 for the case of $\bar{c} = 1.0$. Normal stresses at the edge, $\sigma_y(\bar{x}, 0, 0)$ and at a depth into the plate, $\sigma_y(\bar{x}, \bar{y} = 1, 0)$ are shown in the figure. In Fig. 4, values for the transverse normal stresses at the center of the edge of the sheet are shown for $\bar{c}$ values of 0.5, 1.0, 2.0, and 5.0.

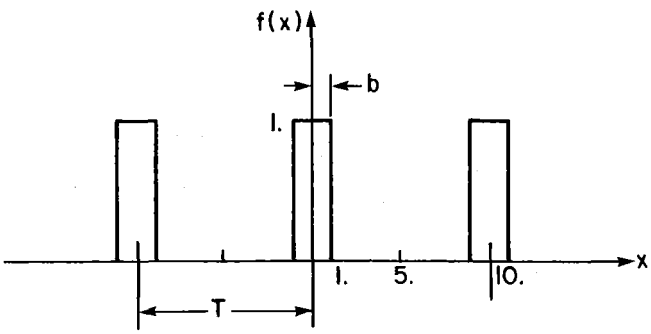

Fig. 2 Periodic system approximated by a Fourier series

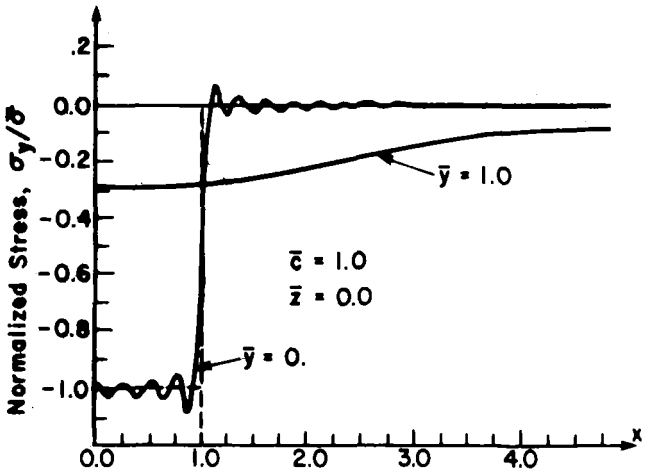

Fig. 3 Stress distribution for σ_y at $y = 0$ and $y = 1.0$

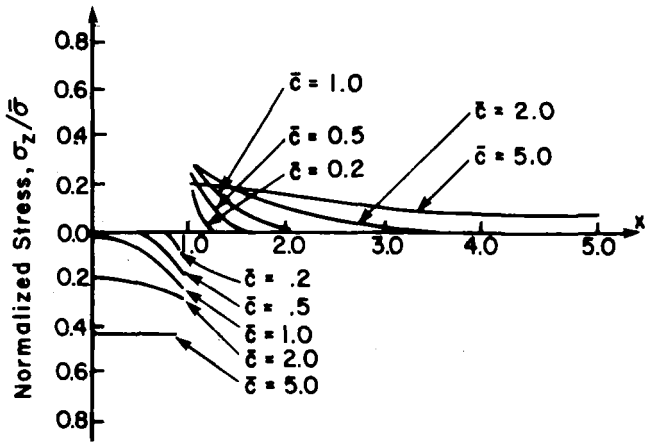

Fig. 4 Stress distribution for σ_z at $y = 0$ and $z = 0$

An important aspect of this solution is the development of transverse normal stresses within the sheet. These stresses are compressive in areas beneath the indentor with a transition to tensile stress beyond the indentor. The aspect ratio, defined as the ratio of indentor width to plate thickness, significantly influences the magnitude of the transverse stresses, as shown in Fig. 4. Maximum transverse normal stresses occur at the center of the edge of the plate.

The magnitude of tensile stresses are not critical for a Von Mises-type material because such materials have equal tension and compression strengths. However, for material which are relatively weak in tension, these transverse normal tensile stresses do influence indentation strength, in some instances markedly. Because of the relative weakness of ice in tension and because tensile failure tends to be more brittle, particularly at higher strain rates, the governing failure mode may be horizontal splitting of the ice sheet. In fact, in particular instances the plane strain indentation strength cannot be achieved because of the transverse splitting. This is in agreement with many experimental findings [15, 16].

Optimum Stress Fields

With a uniform distribution of pressure across the thickness of the plate edge, the outer layers of the sheet are limited to their plane stress indentation strength. Thus, in order to increase the lower bound, a nonuniform distribution of pressure across the edge thickness is necessary. This is possible because the inner layers beneath the indentor are confined. At this point, we take advantage of the lower-bound theorem for which discontinuous stress fields are permitted.

Such a stress field can readily be attained by superimposing on the three-dimensional elasticity solution a plane stress solution in the outer layers of thickness D as shown in Fig. 5. Note that this solution is statically admissible since equilibrium is everywhere maintained including at the plane of discontinuity. The total edge pressure now includes an interior stress level, σ, and an edge stress level, $\sigma - \sigma_o$.

The lower-bound solution now involves numerically optimizing the total indentation pressure with respect to D and σ_o. In the following section, the material stress state is allowed to just reach yield and thus the lower bound values may be the collapse values.

There is, of course, no limit to the number of steps permitted in the applied pressure intensity. It was found that combining a uniaxial compression stress of σ_o' directly below the indentor with the stress field shown in Fig. 6 gives an improved lower bound. This configuration is used to optimize the indentation pressures discussed in the following section. Indentation pressures are calculated and numerically optimized for values of σ_o, σ_o', and σ_o''.

Lower-Bound Solutions

The Von Mises yield criterion is first used to study the effect of aspect ratios on the indentor pressures. Results are shown in Fig. 7 in which the pressures are normalized with respect to the unconfined compression strength. The results compare very well with upper-bound solutions obtained by Croasdale et al. [17].

Frederking and Gold [18] conducted tests to investigate the effects of aspect ratio on indentation pressures. Their tests were conducted using constant rates of indentation. As suggested by Michel and Toussaint [19], an empirical relation for the effective constant strain rate $\dot{\epsilon}$ can be used

$$\dot{\epsilon} = \frac{V}{8b} \tag{15}$$

where V is the indentation velocity and b is the indentation half-width. By using equation (15) and normalizing the results with respect to the uniaxial compression strength for the appropriate effective strain rate, the data points in Fig. 7 are obtained.

The numerical results compare very well with the adjusted

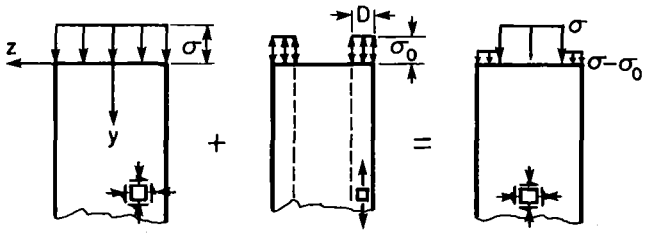

Fig. 5 Discontinuous stress field obtained by superposition

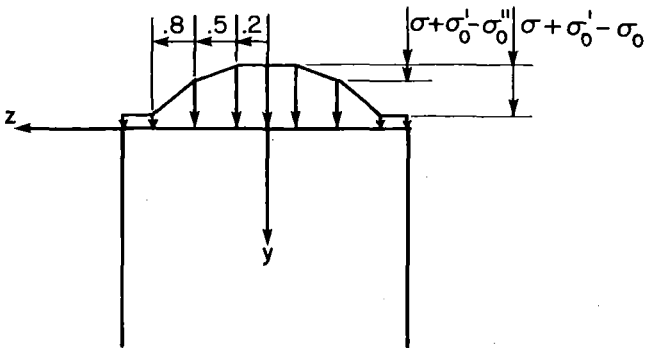

Fig. 6 Improved stress field for optimization

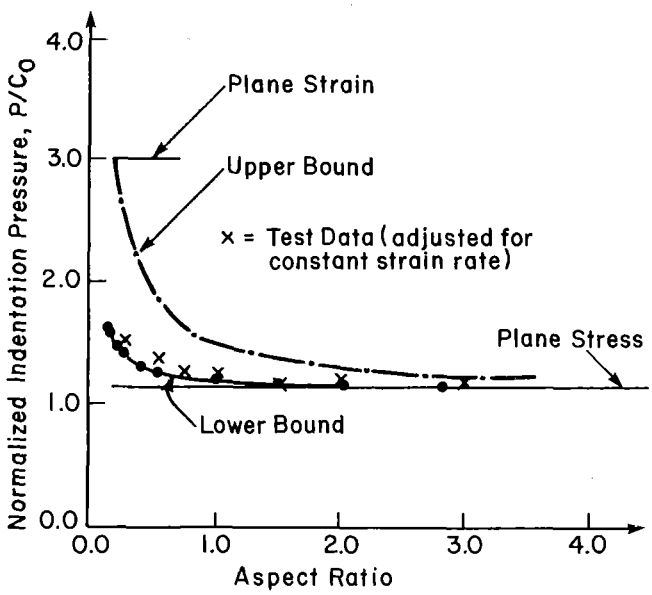

Fig. 7 Normalized indentation pressures using the Von Mises yield criterion

experimental data. The effective strain rates were of the order of 10^{-7} s^{-1}. For these relatively low strain rates, the Von Mises criterion evidently adequately reflects the ice failure. This is not true in general however because at higher strain rates the compression strength/tension strength ratios vary significantly.

As can be seen in the figure, only when the aspect ratio is less than 1.0 does the aspect ratio significantly affect the indentation pressure for a constant effective strain rate. For constant indentation velocity, however, the effect of the aspect ratio is more significant because the effective strain rate (and therefore the ice strength) changes as a function of aspect ratio.

At higher strain rates, the relative weakness of ice in tension must be addressed. To study this effect, the Drucker-Prager criterion is used to calculate indentation pressures. Results are presented in Fig. 8 for various values of α of equation (3). Note that a particular value of α defines the relative tensile strength, T, and relative confined compression strength, R. Also shown in the figure are results from previous two-dimensional indentation solutions [20].

Some interesting aspects of the three-dimensional nature of the indentation problem are reflected in the figure. As α increases, the tensile strength of the material decreases. For aspect ratios near 1.0, significant transverse normal stresses, σ_z, develop but decrease as the aspect ratio decreases (Fig. 4). Smaller aspect ratios are required for indentation pressures to increase for larger values of α (smaller tensile strengths). Also, as α increases, the confined compression strength increases resulting in increased values for the plane stress indentation pressures. It is apparent from this figure that the transition from plane stress to plane strain is highly dependent upon the tensile strength of the sheet.

Results using the anisotropic yield criterion of equation (5) are presented in Fig. 9. Strength parameters suggested by Ralston [21] were used where $\tilde{a}_1 = 1.77$, $\tilde{a}_3 = 3.57$, and $\tilde{a}_9 = -3.54$. The strength parameter $\tilde{a}_9$ reflects the effect of σ_z on material yield. This parameter governs the transition from two-dimensional plane strain conditions. This is also shown in the figure by results for $\tilde{a}_9 = 1.0$. Also shown in the figure are the results from Michel and Toussaint [19] for strain rates of $\dot{\epsilon} = 2.5 \times 10^{-4}$ s^{-1}. At this strain rate level tension and compression strength vary significantly.

Qualitatively, the results are very similar to the results using the Drucker-Prager criterion. In both cases, the indentation

pressures do not exceed the plane stress values unless the aspect ratio is well below 2.0. Solutions rapidly approach the plane strain values for aspect ratios below approximately 0.2. This transition is highly dependent on the yield function used and is extremely sensitive to the tensile strength of the ice medium.

To demonstrate the dependency of indentation pressures on transverse tensile strength, yield criteria discussed by Timco and Frederking [10] are employed. The coefficients of equation (5) can be established by requiring proper reflection for the following strengths: (*a*) uniaxial compression strength in the x (or y) direction; (*b*) uniaxial compression strength in the z direction; (*c*) confined compression strengths in the x-y plane; (*d*) shear strength in the x-y plane; and (*e*) shear strength in the x-z (or y-z) plane.

The following coefficients are thus obtained for discontinuous columnar grained ice at −13°C at a strain rate of 2×10^{-4} s^{-1}: $a_1 = 1.2$ MPa^{-2}, $a_3 = $ MPa^{-2}, $a_4 = 3.2$ MPa^{-2}, $a_7 = 3.9$ MPa^{-1} and $a_9 = 7.7$ MPa^{-1}. The corresponding tensile strength in the z direction normalized with respect to the uniaxial compressive strength in the x direction is $T_z = 0.03$. The calculated indentation pressures for various aspect ratios are presented in Fig. 10. Note that this very low tensile strength prohibits any increase in indentation pressures above the plane stress values (unless $\bar{c} < 0.2$).

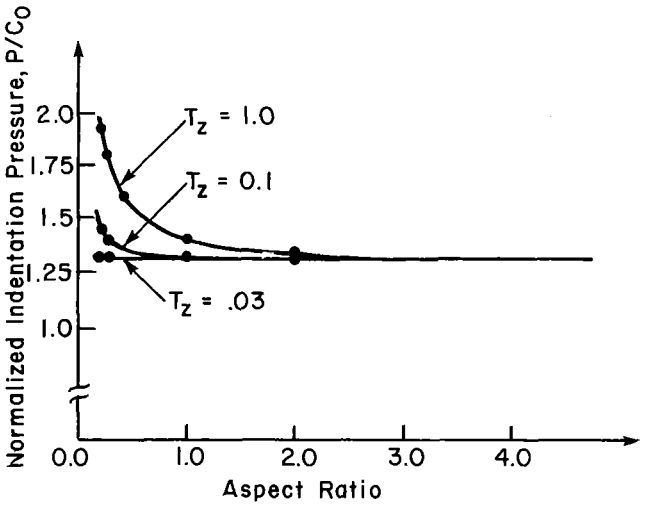

Fig. 10 Normalized indentation pressures for discontinuous columnar grained ice

Also shown in the figure are results for $T_z = 0.18$ and $T_z = 1.0$. The corresponding failure criteria coefficients are found by maintaining the same uniaxial and confined compression strength conditions (*a*), (*b*), and (*c*) mentioned previously. The tensile strengths are varied by changing only the shear strengths, conditions (*d*) and (*e*). Note that by increasing T_z to 0.1, an increase in indentation pressure becomes significant as c becomes less than about 0.5. When $T_z = 1.0$, increases in indentation pressure become appreciable as c becomes less than 1.0. It is evident that transverse tensile strength is an important parameter in quantifying indentation pressure for intermediate aspect ratios.

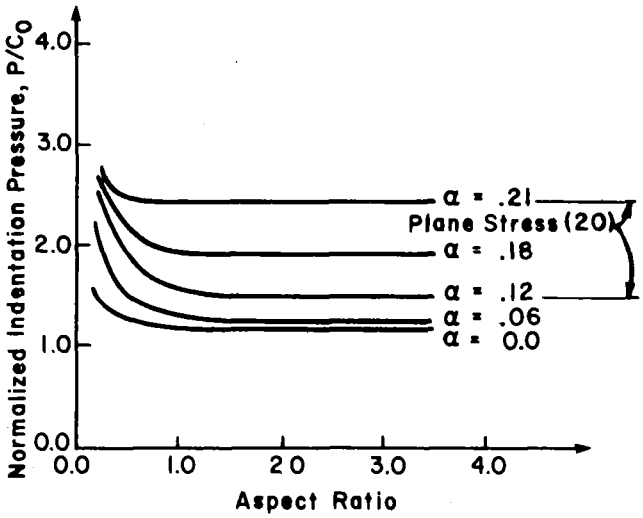

Fig. 8 Normalized indentation pressures using Drucker-Prager criterion

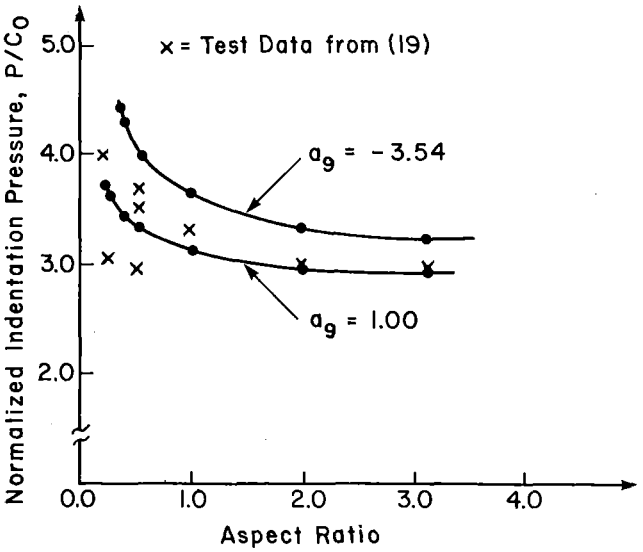

Fig. 9 Normalized indentation pressures using the anisotropic *n*-type yield criterion

Conclusions

To date, most efforts to analytically determine ice indentation pressures using plastic limit analysis have assumed conditions of either plane stress or plane strain. Plane stress results can be considerably higher than the uniaxial compression strength and generally compare favorably with carefully controlled experimental results for higher aspect ratios. For the analysis of plane strain conditions, it is assumed that the necessary transverse normal compressive stresses exist and comparison with experimental results is somewhat less favorable.

A three-dimensional analysis provides a method for describing the stress state of the indented medium for arbitrary aspect ratios. Elasticity solutions indicate that significant transverse tensile stresses result as the plane strain conditions are approached. The failure mechanism for intermediate aspect ratios may therefore be transverse horizontal splitting for lower aspect ratios and the plastic limit pressure for plane strain indentation conditions may not be an adequate approximation.

In contrast to two-dimensional indentation studies, the indentation pressures are shown to be highly dependent upon tensile strength. In order to predict ice indentation pressures for intermediate aspect ratios, it is important to properly establish the ice strength characteristics in the tensile, tensile/compression, and the compression/compression regimes.

Acknowledgment

Support for this study provided by the National Science Foundation through Grant No. CEE-8404687 to the Massachusetts Institute of Technology is gratefully acknowledged.

References

1 Weeks, W. F., and Anderson, D. L., "The Mechanical Properties of Ice," *C.R.E.E.L., Cold Regions Science and Engineering: Part II—Physical Science*, Section C: "Physics and Mechanics of Ice," 1967.

2 Fletcher, N. H., *The Chemical Physics of Ice*, Cambridge University Press, 1970.

3 Hill, R., *The Mathematical Theory of Plasticity*. Oxford University Press, London, 1950.

4 Timoshenko, S., and Goodier, J., *Theory of Elasticity*, McGraw-Hill, New York, N.Y., 1970.

5 Hawkes, I., and Mellor, M., "Deformation and Fracture of Ice Under Uniaxial Stress," *Journal of Glaciology*, Vol. 11, No. 61, 1972, pp. 103–131.

6 Drucker, D. C., and Prager, W., "Soil Mechanics and Plastic Analysis of Limit Design," *Quarterly of Applied Mathematics*, No. X, 1952, pp. 157–165.

7 Reinicke, K. M., and Ralston, T. D., "Plastic Limit Analysis with an Anisotropic, Parabolic Yield Function," *International Journal of Rock Mechanics, Mining Sciences and Geomechanics*, Abstracts, Vol. 14, 1977, pp. 147–154.

8 Paul, B., "Macroscopic Criteria for Plastic Flow and Brittle Failure," *Fracture: An Advanced Treatise*, ed., H. Liebowitz, Vol. II, Academic Press, New York, 1968, pp. 313–496.

9 Ralston, T. D., "Yield and Plastic Deformation in Ice Crushing Failure," Workshop on the Mechanical Properties of Ice, Alberta, Canada, 1977.

10 Timco, G. W., and Frederking, R. M. W., "An Investigation of the Failure Envelope of Granular/Discontinuous—Columnar Sea Ice," *Cold Regions Science and Technology*, Vol. 9, 1984, pp. 17–27.

11 Chen, W. F., *Limit Analysis and Soil Plasticity*, Elsevier Press, Amsterdam, 1975.

12 Drucker, D. C., Prager, W., and Greenberg, H. J., "Extended Limit Design Theorems for Continuous Media," *Quarterly of Applied Mathematics*, Vol. IX, 1952, pp. 381–389.

13 Clark, R. A., and Reissner, E., "A Tenth-Order Theory of Stretching of Transversely Isotropic Sheets," *Journal of Applied Mathematics and Physics*, Vol. 35, 1984, pp. 883–889.

14 Clark, R. A., "Three-Dimensional Corrections for a Plane Stress Problem," *International Journal of Solids and Structures*, Vol. 21, No. 1, 1985, pp. 3–10.

15 Schwarz, J., Hirayamam, K., and Wu, H. C., "Effect of Ice Thickness on Ice Forces," OTC Paper No. 2048, 1974.

16 Zabilansky, L. J., Nevel, D. E., and Haynes, F. D., "Ice Forces on Model Structures," *Canadian Journal of Civil Engineering*, Vol. 2, No. 400, 1975, pp. 400–417.

17 Croasdale, K. R., Morgenstern, N. R., and Nuttall, J. B., "Indentation Tests to Investigate Ice Pressures on Vertical Piers," *Journal of Glaciology*, Vol. 19, No. 81, 1977.

18 Frederking, R., and Gold, L. W., "Experimental Study of Edge Loading of Ice Plates," *Canadian Geotechnical Journal*, No. 12, 1975, pp. 456–463.

19 Michel, V., and Toussaint, N., "Mechanisms and Theory of Indentation of Ice Plates," *Journal of Glaciology*, Vol. 19, No. 81, 1977.

20 Karr, D. G., and Das, S. C., "Limit Analysis of Ice Sheet Indentation," ASME *Journal of Energy Resources Technology*, Vol. 105, Sept. 1983, pp. 352–355.

21 Ralston, T. D., "An Analysis of Ice Sheet Indentation," *Fourth International Symposium on Ice Problems*, I.A.H.R., 1978.